Available online at www.sciencedirect.com
SCIENCE DIRECT®
Biochemical and Biophysical Research Communications 304 (2003) 153–159
BBRC
www.elsevier.com/locate/ybbrc

Effect of phospholipase Cβ4 lacking in thalamic neurons on electroencephalogram

Miho Kameyama,[a] Isao Yamaguchi,[b] Kazuhisa Ichikawa,[b,c] Takashi Sugiyama,[a,1] Moritoshi Hirono,[a,2] Hirokazu Hori,[d] Masayuki Ikeda,[e] Yuko Kuwahata,[e] Naomi Eguchi,[e] Yoshihiro Urade,[e] and Tohru Yoshioka[a,*]

[a] *Department of Molecular Neurobiology, School of Human Sciences, Waseda University, Tokyo 169-8555, Japan*
[b] *Brain Information Science Laboratory, Corporate Research Laboratories, Fuji Xerox Co., Ltd., Kanagawa 259-0157, Japan*
[c] *Advanced Research Center for Science and Engineering, Waseda Univeristy, Tokyo 169-8555, Japan*
[d] *Department of Electrical Engineering, Faculty of Engineering, Yamanashi University, Kofu 400-851, Japan*
[e] *Department of Molecular Behavioral Biology, Osaka Bioscience Institute, Osaka 565-0874, Japan*

Received 28 February 2003

Abstract

Activity of thalamic neurons has been shown to be modulated via type-1 metabotropic glutamate receptor (mGluR1) activation, which initiates an intracellular Ca signaling cascade involving phospholipase Cβ4 (PLCβ4) and leading to the activation of conventional protein kinase C (cPKC). In the present study, we investigated the role of PLCβ4 in thalamic neuron. PLCβ4-deficient mutant mice were found to exhibit three phenotypic characteristics: (1) a 2-Hz increase in the peak frequency of electroencephalogram (EEG) of rapid eye movement (REM) sleep, (2) an increase in the frequency of miniature excitatory postsynaptic currents (mEPSCs) recorded in thalamus, and (3) waveform distortion of EEG. We postulate here that changes in protein phosphorylation due to reduced cPKC activity by PLCβ4 deletion in thalamic neurons may give rise to these phenotypic characteristics. Taken together, these results indicate that reduced PLCβ4 activity in thalamic neurons may underlie high-cortical oscillation frequency.

Keywords: PLCβ4; Thalamus; LGNd; EEG; mEPSC; FFT; PST; Mouse

It was previously reported that PLCβ4 plays important roles in the phototransduction in vertebrate photoreceptors in retina [1] and in the eye blink reflex conditioning induced by Purkinje cells in cerebellum [2,3]. In these cases signaling cascades initiated by the activation of mGluRs were found to activate PKCα/β1.

Since PLCβ4 is localized in the thalamus, we attempted to analyze sleeping state of the mouse. Sleep/waking states are associated with two types of cortical oscillation patterns of EEG in the thalamus, delta waves, and spindles, but the underlying mechanisms are not clearly understood. Delta waves (0.5–4 Hz) likely arise from the activity of thalamocortical neurons. These neurons generate rhythmic bursts of action potentials in the frequency range of delta waves [4]. Spindles arise from both intrinsic and network activities in the thalamus [5]. The generation of spindle rhythmicity (7–14 Hz) involves interactions between thalamic reticular and thalamocortical neurons [6,7]. Based on this hypothesis, Golomb et al. [8] proposed that a model network of isolated thalamic reticular neurons oscillates spontaneously, and the frequency of the model network is regulated primarily by thalamocortical neurons. Therefore it is reasonable to assume that PLCβ4 deleted mouse will provide some effect on the EEG in the sleep.

In the present study, we investigated the effects of PLCβ4 deletion on EEG in the waking state, slow-wave

* Corresponding author. Present address: Room 601, Bldg. 66, Waseda University, 3-14-9, Okubo, Shinjuku-ku, Tokyo 169-0072, Japan. Fax: +81-3-3205-6419.
E-mail address: yoshit@waseda.jp (T. Yoshioka).
[1] Present address: Olympus Optical Co., Ltd., Tokyo 192-8512, Japan.
[2] Present address: Vollum Institute, Oregon Health Science University, 3181, SW Sam Jackson Park Road, Portland, OR 97201, USA.

0006-291X/03/$ - see front matter © 2003 Elsevier Science (USA). All rights reserved.
doi:10.1016/S0006-291X(03)00536-9

sleep, and REM sleep. We examined this immunohistochemically and electrophysiologically and found that PLCβ4-deficient mutant mice exhibited a clear effect on cortical oscillation during REM sleep.

Materials and methods

Generation of PLCβ4-deficient mutant mice. Mice with a disruption of the PLCβ4 gene were generated in the laboratory of M. Katsuki according to standard methods [9]. A genomic clone encoding the PLCβ4 catalytic region was isolated to construct a targeting vector in which exons that encode amino acid residues 539–646 were replaced with a neomycin-resistant gene cassette, and a diphtheria toxin fragment A gene was attached to the targeting vector for negative selection [2]. Male chimeric mice were bred with C57BL/6J female mice. The tail DNA of offspring was analyzed using Southern blot analysis to identify the genotype or amplified using polymerase chain reaction (PCR).

Immunohistochemistry. At the third or fourth postnatal week, mice were deeply anesthetized using pentobarbital (4 mg/100 g) and transcardially perfused with 4% phosphate-buffered paraformaldehyde (4 °C; pH 7.4). The brains were dissected out, immersed in the same fixative for approximately 12 h, and then embedded in paraffin. Sagittal or coronal paraffin-embedded sections (3–5 μm thick) were prepared for immunohistochemical visualization using a streptavidin-peroxidase reaction (Nichirei, Japan) [10,11].

In PLCβ4-deficient mouse no immunostaining was observed in thalamus as well as in celleberum [3]. The same sections were stained with cresyl violet for Nissl staining.

Western blot analysis. Coronal slices (400 μm) containing the geniculate nucleus and hippocampus were made using a vibration slicer in ice-cold high-Mg^{2+} artificial cerebrospinal fluid (ACSF) containing (mM) 138.6 NaCl, 3.35 KCl, 21 $NaHCO_3$, 0.6 NaH_2PO_4, 9.9 d-glucose, 0.5 $CaCl_2$, and 4 $MgCl_2$, bubbled with 95% O_2/5% CO_2. The ventral lateral geniculate nucleus (LGNv), medial geniculate nucleus (MGN), dorsal lateral geniculate nucleus (LGNd), and hippocampus (dentate and CA3 region) were dissected from wild-type ($n = 3$) and PLCβ4-deficient mutant mice ($n = 3$). These samples were homogenized and 5 μg of protein was separated using 7.5% SDS–polyacrylamide gel electrophoresis. Separated proteins were transferred to nitrocellulose membranes. The membrane was incubated with anti-PLCβ1, -β2, -β3, and -β4 antibodies (1/1000 dilution; Santa Cruz Biotechnology) and then with alkaline-phosphate-labeled secondary antibody (1/5000 dilution; Promega). Immunoreacted bands were visualized using ProtoBlot Western Blot AP Systems (Promega).

EEG and EMG recording. Adult (10–12 weeks old) PLCβ4-deficient mutant male mice ($n = 4$) and wild-type control mice ($n = 6$) were used in the experiments. The animals were maintained at a 12-h light/dark cycle (light from 8 a.m. to 8 p.m.) in sound-attenuate, temperature-controlled (22.0 ± 1.0 °C) chambers. Under pentobarbital anesthesia (50 mg/kg, i.p.), mice were implanted with EEG and electromyograph (EMG) electrodes for polysomnographic recordings. For monitoring EEG signals, two stainless steel screws were placed through the skull over the cortex (2.0 mm posterior and 2.5 mm to the right from bregma, 1.5 mm posterior from lambda). The EEG and EMG were recorded using a swivel and slip ring wire apparatus, designed so that the mice could move without any restriction.

After a 10-day recovery period, the sleep/waking states of the mice were monitored for a period of 48 h, which comprised baseline and experimental days. The EEG and EMG signals were amplified and filtered (EEG, 0.5–30 Hz; EMG, 20–200 Hz), digitized at a sampling rate of 128 Hz, and recorded using a data acquisition program SLEEPSIGN as described previously [12].

Ca^{2+} imaging. Coronal slices (200 μm) containing the geniculate nucleus and hippocampus were prepared using a vibration slicer with the tissue submerged in ice-cold high-Mg^{2+} ACSF, bubbled with 95% O_2/5% CO_2. The slices were incubated for 1–3 h in ACSF containing 2.5 mM $CaCl_2$ and 1 mM $MgCl_2$, bubbled with 95% O_2/5% CO_2, and then transferred for 1 h to ACSF containing 10 μM fura-2 AM (Molecular Probes) and 0.001% Cremophore E1 (Sigma) at room temperature. The intensity ratio (F340 nm/F380 nm) was analyzed using a digital imaging system (Argus-50CA, Hamamatsu Photonics). The imaging methods have been described in more detail previously [13].

Patch clamp electrophysiology. Thalamic geniculate slices were prepared by the same methods as for the Ca^{2+} imaging experiment. Whole-cell voltage-clamp recordings were made from visually identified [14] neurons (15–25 μm) under Nomarski optics using a water-immersion objective (Achroplan 63×/0.90 w, Zeiss, Germany).

EEG analysis. The raw EEG data were subjected to the fast Fourier transform (FFT) [15] and the phase space trajectory (PST) analysis. The PST analysis is generally used to extract the characteristics of oscillatory waveforms [16]. Thus, we applied the PST analysis to figure out characteristics of the EEGs. The PSTs of the EEGs were made by plotting the amplitude of EEG ($V(t)$) on the x-axis and the velocity of the voltage change (the first differential of amplitude for time t: $dV(t)/dt$) on the y-axis. Plotting areas for $V(t)$- and $dV(t)/dt$-axis were set in the range within ±0.8 and ±50 mV/s, respectively. These theoretical analyses were performed for a randomly selected period of 12 s from 48 h recordings for three states (waking, slow-wave sleep, and REM sleep).

During the course of the present study, the care of the animals conformed to the guidelines established by the Institutional Animal Investigation Committee at the University of Tokyo.

Results and discussion

The distribution of PLCβ4 in whole mouse brain was examined using an antibody for PLCβ4. PLCβ4 was primarily located in cerebellum, olfactory bulb, and the thalamic geniculate nuclei as it was reported previously [1,3]. At higher magnification, we observed dense staining in the LGNd and MGN (Fig. 1A). Higher magnification of LGNd revealed intense staining of neurons specifically, evenly distributed throughout the structure (Fig. 1B).

Interestingly, PLCβ4 staining was not observed in the hippocampus (Fig. 1A). The distribution of other subtypes of PLCβ was also examined. PLCβ1 was detected slightly in the thalamic geniculate nuclei (immunohistochemical data not shown). PLCβ3 was detected only in the Western blotting slightly (Fig. 1D). No staining for PLCβ4 was detected in PLCβ4-deficient mutant mice (Fig. 1C).

Calcium mobilization in response to exposure to DHPG (100 μM) was robust in neurons in acute slices of LGNd from wild-type mice, while that from PLCβ4-deficient mutant mice was markedly reduced (Figs. 2A and C) ($n = 5$). No effect of TTX on DHPG-induced Ca^{2+} mobilization was observed. High-K^+ stimulation induced a higher Ca^{2+} elevation in PLCβ4-deficient mutant mice than wild-type mice (Fig. 2C) ($n = 7$). As a control experiment, neurons in the dentate gyrus (DG) in hippocampus were examined under the same conditions as those in the LGNd. No difference in Ca^{2+} mobilization was observed between hippocampal neurons from wild-type mice and those

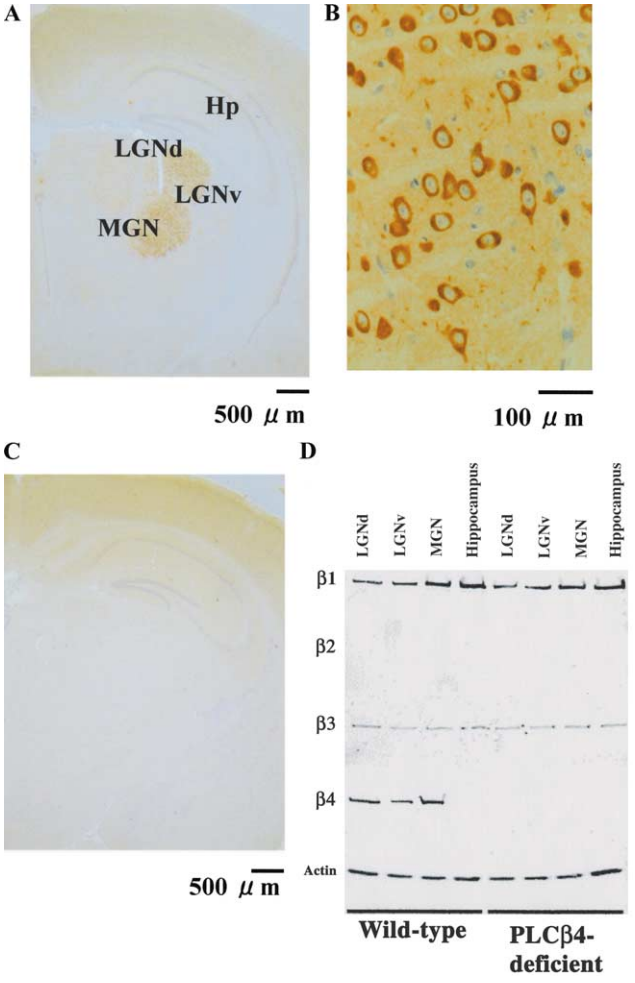

Fig. 1. Localized immunostaining for PLCβ4 in mouse brain. (A) Immunostaining of the thalamus and hippocampus (Hp) of a wild-type mouse with anti-PLCβ4 antibody. Localized immunoreactivity was found in the MGN and LGNd. The LGNv had less immunoreactivity. No immunoreactivity was observed in hippocampus, but it was identified using counter-staining with cresyl violet. (B) Higher magnification of thalamic neurons of a wild-type mouse stained with anti-PLCβ4 antibody. The soma of thalamic neurons exhibited immunoreactivity for anti-PLCβ4 antibody, but the nucleus itself was not stained at all. Stained areas without white nuclei were cells sliced out of the plane of the nucleus. Blue spots without antibody staining may be another type of cell, such as glia. (C) PLCβ4-deficient mutant mouse was not stained by anti-PLCβ4 antibody at all. (D) The distribution of PLCβ families was confirmed using the Western blotting technique. Actin was used as the control.

from PLCβ4-deficient mutant mice (Fig. 2B). The reduced DHPG-stimulated Ca^{2+} mobilization observed in the thalamus of PLCβ4-deficient mutant mice suggests that the lack of PLCβ4 impaired mGluR1-initiated intracellular Ca^{2+} mobilization. In contrast, Ca^{2+} elevation in response to high-K^+ stimulation was higher in PLCβ4-deficient mutant mice than in wild-type mice. This indicates that voltage-sensitive Ca^{2+} channels and/or K^+ channels may be modulated by an intracellular signaling cascade involving PLCβ4, probably via PKC [17].

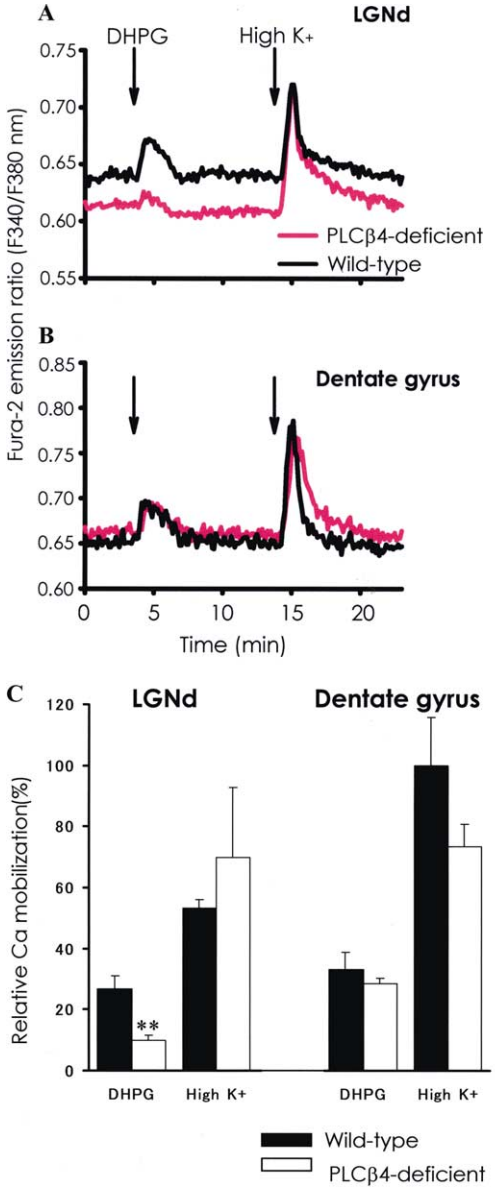

Fig. 2. Ca^{2+} mobilization in both LGNd (thalamus) and Dentate gyrus (hippocampus) slices from wild-type and PLCβ4-deficient mutant mice. (A) The time course of Ca^{2+} levels in LGNd neurons. Ca^{2+} responses to DHPG application were normal in wild-type mice, while the responses disappeared entirely in PLCβ4-deficient mutant mice. Ca^{2+} responses to high-K^+ (50 mM), however, were similar in wild-type and PLCβ4-deficient mutant mice. (B) Ca^{2+} responses to DHPG and high-K^+ were normal in DG neurons from both wild-type and PLCβ4-deficient mutant mice. (C) The relative Ca^{2+} mobilization was calculated as a percent of the 50 mM high-K^+ induced Ca^{2+} response of DG slice in wild-type mice, which is normalized as 100%. Error bar is expressed as mean ± SEM, $n = 5$ for wild-type, $n = 7$ for PLCβ4-deficient mutant mice. $^{**}p < 0.01$ in comparison to wild-type group by Student's t test. In LGNd, PLCβ4-deficient mutant mice showed significantly lower response to DHPG and higher response to high-K^+ stimulation than those of wild-type mice. In DG, PLCβ4-deficient mutant mice showed a similar Ca^{2+} response as wild-type mice.

A comparison of the electrophysiology of neurons in acute slices of thalamus revealed an increase in the frequency of miniature excitatory postsynaptic currents

(mEPSCs) in PLCβ4-deficient mutant mice versus wild-type mice (Fig. 3). The mEPSC of thalamic neuron was recorded for long periods in the presence of TTX. Frequency distribution was plotted for wild-type (Fig. 3C) and PLCβ4-deficient mice (Fig. 3D). The mean decay constants calculated from an exponential curve fit to the mEPSC frequency distribution were tightly distributed around lower values for wild-type mice, while those for PLCβ4-deficient mutant mice exhibited a wide distribution at higher values.

Current hypotheses are based on the idea that increased mEPSC frequency is due to an increase in the amount of neurotransmitter release from the presynaptic terminal and that enhanced mEPSC amplitude is due to the modulation of AMPA receptors [17]. Effect of PKA and PKC on mEPSC amplitude and frequency in CA1 pyramidal cells was studied by using forskolin and PDBu, respectively [18]. It is likely to assume that PDBu, nonspecific activation of PKC, increase the frequency of mEPSC. Although the result seems contrary to ours, it might be due to the nonspecific activation of PKC in the hippocampus. Caution must be paid to the fact that PLCβ4 does not exist in the neuron of hippocampus. On the other hand, it was reported that activation of mGluR1 resulted in presynaptic inhibition of glutamate release from retinal afferent and seems likely from cortical afferent [19].

Therefore, the results of the present study can be explained by the idea that the increase in mEPSC

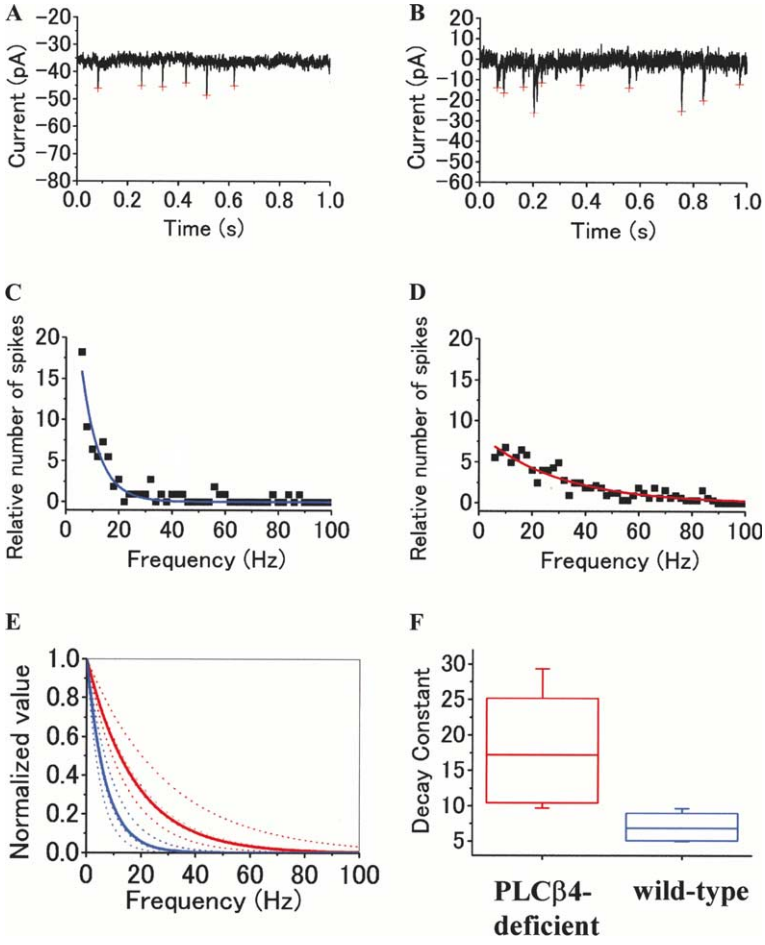

Fig. 3. Frequency distribution of mEPSCs recorded from thalamic slices from wild-type and PLCβ4-deficient mutant mice. (A) Representative mEPSCs (marked by cross bars) recorded from an acute slice of thalamus from a wild-type mouse. (B) Representative mEPSCs recorded from a thalamic slice from a PLCβ4-deficient mutant mouse. (C) Number of mEPSCs plotted against frequency ($1/\Delta t$; Δt is the interval between mEPSCs) for a representative wild-type mouse. The mEPSC frequency distribution was fitted by a single exponential decay curve (solid line). (D) Number of mEPSCs plotted against $1/\Delta t$ for a PLCβ4-deficient mutant mouse. (E) The mean decay constants (blue and red solid lines) were calculated for the mEPSC frequency distribution for both wild-type (blue broken lines) and PLCβ4-deficient mutant mice (red broken lines). The decay constant τ is defined by this equation: $f(x) = A\exp(-x/\tau)$; x is the frequency and A is the arbitrary number. The mean decay constant for the exponential decay curve for PLCβ4-deficient mutant mice (red solid line) was higher than that for wild-type mice (blue solid line). (F) Mean values for decay constants for wild-type and PLCβ4-deficient mutant mice. Upper and lower horizontal bars indicate the maximal and minimal data, respectively. Upper and lower horizontal lines correspond to the standard deviation and the middle lines correspond to the median value. The decay constant for PLCβ4-deficient mutant mice ($n = 5$) was significantly larger than that for wild-type mice ($n = 4$; $p = .026$; Student's t test).

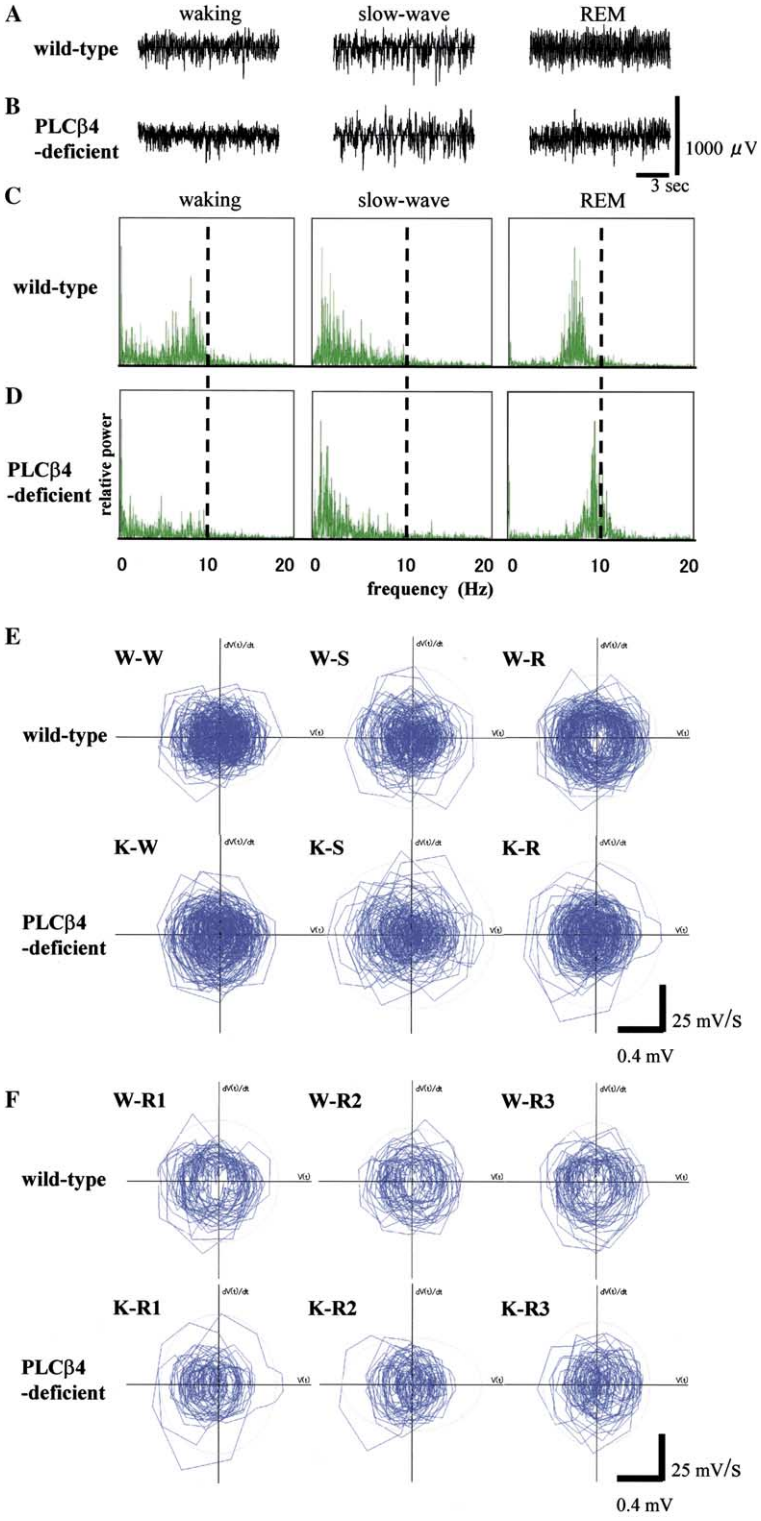

Fig. 4. EEG, the frequency power spectra, and PST for wild-type and PLCβ4-deficient mutant mice. Representative EEG recordings for REM sleep, slow-wave sleep, and waking in wild-type (A) and PLCβ4-deficient mutant (B) mice. Representative power spectra for REM, slow-wave sleep, and waking in wild-type (C) and PLCβ4-deficient mutant (D) mice. During REM sleep, PLCβ4-deficient mutant mice exhibited a 2-Hz increase in the peak frequency compared to wild-type mice. In the waking state, PLCβ4-deficient mutant mice did not exhibit the peak around 7 Hz observed in wild-type mice. PST for waking (W), slow-wave sleep (S), and REM sleep (R) for a 12 s period (E). Calculation was carried out for the same EEG recordings shown in (A, B). *x*- and *y*-axes of the coordinate are expressed with absolute values. Twelve second trajectory pattern of REM sleep for wild (W-R) and knock-out mice (K-R) was divided into three parts (F) in order to elucidate the fluctuation of the trajectory pattern in 12 s. In wild type, each pattern has a vacancy in the center of the circle, although small fluctuations are present (W-R1, -R2, and -R3). There is no vacancy in the center of trajectory pattern for the knock-out mice (K-R1, -R2, and -R3).

frequency may be due to a reduction in mGluR1 signaling activity in the presynaptic terminal.

A FFT was applied to the raw EEG recording (Figs. 4A and B) to yield the power spectra (Figs. 4C and D). For wild-type mice, the REM-sleep power spectrum was symmetrically distributed around 7.2 Hz (Fig. 4C). For PLCβ4-deficient mutant mice, the REM-sleep power spectrum was symmetrically distributed around 9.2 Hz (Fig. 4D). In the slow-wave-sleep power spectrum, most frequencies were in the lower frequencies. The power spectrum in the waking state had many components in the middle range (1–7 Hz) and a small peak around 7 Hz. The power spectra in slow-wave sleep and waking state of knock-out mice were also similar to those for wild-type mice.

The smaller difference between wild and knock-out mice observed in frequencies around 7–10 Hz during the waking state may be due to differences in the flow of sensory information from the thalamus to the cerebral cortex [20]. It is likely that the higher frequency of mEPSCs underlies the higher frequency of EEG power spectra in the REM sleep observed in PLCβ4-deficient mutant mice. This difference can be ascribed to an interruption in the mGluR1-mediated intracellular signaling cascade in the thalamus.

In order to extract more information from EEG, we attempted to apply PST analysis, which is efficient to detect irregular waveforms in EEG, because the trajectory pattern describes relationships between amplitude of waveform of EEG ($V(t)$) and its first differential with t ($\mathrm{d}V(t)/\mathrm{d}(t)$) (Figs. 4E and F). If $V(t)$ is sinusoidal, trajectory pattern will show a circular pattern. Interestingly, only EEG in REM-sleep state showed a clear difference between wild-type and PLCβ4-deficient mutant mice. A PST for 12 s length of EEG recordings in REM sleep of wild-type showed a vacancy in the center of the PST circles, while no observable vacancy was present in the PST of PLCβ4-deficient mutant (Fig. 4E W-R, K-R). Such a ring pattern in wild-type was maintained even when the EEG data for 12 s were divided into 3 parts of 4 s each (Fig. 4f W-R1, W-R2, and W-R3). The PST for waking/slow-wave-sleep EEG in wild mice showed no vacancy in the center.

The vacant structure observed in REM sleep of wild-type (Fig. 4E) means that there is a limitation in both amplitude and wave shape of EEG in normal REM sleep; EEG in REM sleep is stable in both amplitude and frequency to some extent. The lack of vacancy structure in the REM-sleep PST of PLCβ4-deficient mutant means that this restriction in the REM sleep is removed if PLCβ4 is deleted from LGN, which is also indicated at the foot of power spectra (Fig. 4D). Waveform changes by the deletion of PLCβ4 from thalamic neurons can be detected efficiently by combinations of FFT and PST analysis. Therefore it can be concluded that deletion of PLCβ4 in thalamocortical neurons induced the lack of intracellular Ca^{2+} mobilization by glutamate stimulation, which affected the peak frequency and the waveform of EEG via increase in the frequency of mEPSC. Further study is needed to clarify relationships between PLCβ4 and frequency of mEPSC.

Acknowledgment

This work was supported by Research for the Future Program (96L00310) to T.Y. from Japan Society for the Promotion of Science.

References

[1] D. Kim, K.S. Jun, S.B. Lee, N.G. Kang, D.S. Min, Y.H. Kim, S.H. Ryu, P.G. Suh, H.S. Shin, Phospholipase C isozymes selectively couple to specific neurotransmitter receptors, Nature 389 (1997) 290–293.
[2] Y. Kishimoto, M. Hirono, T. Sugiyama, S. Kawahara, K. Nakao, M. Kishio, M. Katsuki, T. Yoshioka, Y. Kirino, Impaired delay but normal trace eyeblink conditioning in PLCβ4 mutant mice, Neuroreport 12 (2001) 2919–2922.
[3] M. Hirono, T. Sugiyama, Y. Kishimoto, I. Sakai, T. Miyazawa, M. Kishio, H. Inoue, K. Nakao, M. Ikeda, S. Kawahara, Y. Kirino, M. Katsuki, H. Horie, Y. Ishikawa, T. Yoshioka, Phospholipase Cβ4 and protein kinase Cα and/or protein kinase Cβ1 are involved in the induction of long term depression in cerebellar Purkinje cells, J. Biol. Chem. 276 (2001) 45236–45242.
[4] F. Amzica, M. Steriade, Short- and long-range neuronal synchronization of the slow (<1 Hz) cortical oscillation, J. Neurophysiol. 73 (1995) 20–38.
[5] M. Steriade, R.R. Llinas, The functional states of the thalamus and the associated neuronal interplay, Physiol. Rev. 68 (1988) 649–742.
[6] M. Steriade, E.G. Jones, R.R. Llinas, Thalamic Oscillations and Signaling, Wiley, New York, 1990.
[7] M. Steriade, D.A. McCormick, T.J. Sejnowski, Thalamocortical oscillations in the sleeping and aroused brain, Science 262 (1993) 679–685.
[8] D. Golomb, X.J. Wang, J. Rinzel, Synchronization properties of spindle oscillations in a thalamic reticular nucleus model, J. Neurophysiol. 72 (1994) 1109–1126.
[9] M.R. Capecchi, Altering the genome by homologous recombination, Science 244 (1989) 1288–1292.
[10] J.L. Guesdon, T. Ternynck, S. Avrameas, The use of avidin–biotin interaction in immunoenzymatic techniques, J. Histochem. Cytochem. 27 (1979) 1131–1139.
[11] R. Warnke, R. Levy, Detection of T and B cell antigens hybridoma monoclonal antibodies: a biotin–avidin–horseradish peroxidase method, J. Histochem. Cytochem. 28 (1980) 771–776.
[12] E. Pinzar, Y. Kanaoka, T. Inui, N. Eguchi, Y. Urade, O. Hayaishi, Prostaglandin D synthase gene is involved in the regulation of non-rapid eye movement sleep, Proc. Natl. Acad. Sci. USA 97 (2000) 4903–4907.
[13] M. Ikeda, T. Sugiyama, K. Suzuki, T. Moriya, S. Shibata, M. Katsuki, C.N. Allen, T. Yoshioka, PLCβ4-independent Ca^{2+} rise via muscarinic receptors in the mouse suprachiasmatic nucleus, Neuroreport 11 (2000) 907–912.
[14] C. Chen, W.G. Regehr, Developmental remodeling of the retinogeniculate synapse, Neuron 28 (2000) 955–966.
[15] R.K. Otnes, L. Enocson, Applied Time Series Analysis, Wiley, New York, 1978.
[16] H. Haken, Synergetics, second enlarged ed., Springer, Berlin, Heidelberg, New York (1978).

[17] R. Anwyl, Metabotropic glutamate receptors: electrophysiological properties and role in plasticity, Brain Res. Brain Res. Rev. 29 (1999) 83–120.
[18] R.C. Carroll, R.A. Nicoll, R.C. Malenka, Effects of PKA and PKC on miniature excitatory postsynaptic currents in CA1 pyramidal cells, J. Neurophysiol. 80 (1998) 2797–2800.
[19] J. Cirone, C.A. Pothecary, J.P. Turner, T.E. Salt, Group 1 metabotropic glutamate receptors (mGluRs) modulate visual responses in the superficial superior colliculus of the rat, J. Physiol. 541 (2002) 895–903.
[20] D.A. McCormick, T. Bal, Sensory gating mechanisms of the thalamus, Curr. Opin. Neurobiol. 4 (1994) 550–556.